Ambient Occlusion Opacity Mapping for Visualization of Internal Molecular Structure

David Borland
The Renaissance Computing
Institute, USA
borland@renci.org

ABSTRACT

Molecular surfaces often exhibit a complicated interior structure that is not fully visible from exterior viewpoints due to occlusion. In many cases this interior cavity is the most important feature of the surface. Applying standard blended transparency can reveal some of the hidden structure, but often results in confusion due to impaired surface-shape perception. We present ambient occlusion opacity mapping (AOOM), a novel visualization technique developed to improve understanding of the interior of molecular structures. Ambient occlusion is a shading method used in computer graphics that approximates complex shadows from an ambient light source by rendering objects darker when surrounded by other objects. Although ambient occlusion has previously been applied in molecular visualization to better understand surface shape, we instead use ambient occlusion information to determine a variable opacity at each point on the molecular surface. In this manner, AOOM enables rendering interior structures more opaque than outer structures, displaying the inner surface of interest more effectively than with constant-opacity blending. Furthermore, AOOM works for cases not handled by previous cavity-extraction techniques. This work has been driven by collaborators studying enzyme-ligand interactions, in which the active site of the enzyme is typically formed as a cavity in the molecular surface. In this paper we describe the AOOM technique and extensions, using visualization of the active site of enzymes as the driving problem.

Keywords: Molecular visualization, ambient occlusion, transparent surfaces

1 INTRODUCTION

Visualization has become an essential tool for many scientists working with molecular data. Ball-and-stick, ribbon, and surface renderings are all visualization techniques that enable improved understanding of molecular structures [10, 23, 30, 40]. Our collaborators use visualization techniques such as these to study enzyme-ligand interactions.

Enzymes are proteins that catalyze the transformation of a substrate molecule into a product. The substrate/product is often referred to as the "ligand" with which the enzyme binds. Our collaborators use molecular surface renderings to understand the shape of the active site of the enzyme and its spatial relationship to the ligand during binding. The active site is typically a complicated internal cavity that is largely hidden from exterior viewpoints due to occlusion (Figure 2). Two tools commonly used for viewing occluded structures are transparency and clipping planes.

Applying standard blended transparency to the surface reveals some of the internal structure, but often results in impaired surface-shape perception [24]. Clipping planes can also reveal internal structure, but are typically insufficient for displaying complicated
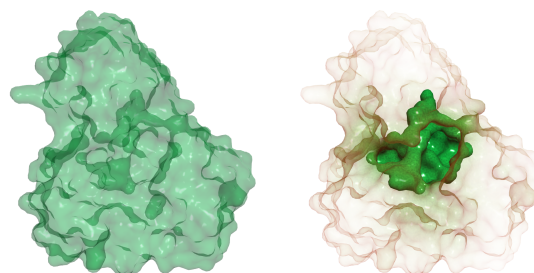
Figure 1: Standard transparency on the left versus ambient occlusion opacity mapping (AOOM) on the right. The structure of the inner cavity, and its context within the outer surface, is easier to understand with AOOM.

non-planar surfaces such as enzyme active sites. Another potential technique that might be used is applying depth-peeling to remove the closest surface to the viewpoint. Such a technique would be inaccurate for this application, however, as the visible portions of the cavity would be removed, and the second surface may not correspond to the cavity in areas of folds and bumps of the outer surface. To enable improved visualization of the active sites of enzymes, we have developed a technique that uses ambient occlusion information to identify and emphasize these hidden structures.

Ambient occlusion is a shading method used in computer graphics that approximates complex shadows from an ambient light source. Surfaces surrounded by objects that block ambient light are rendered

darker than those open to the environment, so ambient occlusion is therefore a measure of the "hiddenness" of an object. Ambient occlusion has been successfully used in molecular visualization to help understand surface shape and identify the locations of cavities in molecular surfaces [39]. Instead of using ambient occlusion information solely for enhancing surface shading, ambient occlusion opacity mapping (AOOM) uses ambient occlusion to calculate a variable opacity at each point on the molecular surface. Because ambient occlusion is a measure of the hiddenness of an object, AOOM can render outer structures more transparent and inner structures more opaque, displaying the inner surface of interest more effectively than with standard transparency (Figure 1). In this paper we apply AOOM to the visualization of enzyme active sites and describe various extensions to the core AOOM technique driven by collaboration with biochemists.

The paper is organized as follows: Section 2 provides background information on the biochemistry our collaborators are studying. Section 3 provides related work in the areas of molecular surface visualization, occlusion and transparency in visualization, and ambient occlusion. Section 4 describes the AOOM implementation, extensions, and supplemental visualization techniques. Section 5 concludes and provides future work.

2   SCIENTIFIC BACKGROUND

Our collaborators study the architecture of the active sites of enzymes involved in the tetrapyrrole biosynthesis pathway. The enzymes in this pathway catalyze reactions involving ligands that are necessary for the formation of various molecules such as hemoglobin, vitamin coenzyme B_{12}, and chlorophyll. Of interest are how different enzyme active-site architectures interact with their respective ligands.

PyMOL, an open-source molecular visualization system (www.pymol.org), is used by our collaborators to visualize ligands bound in the enzyme active sites, with crystallographic data taken from the Protein Data Bank (www.pdb.org). Understanding the active site where the ligand binds with the enzyme is especially important for answering questions such as: a) How much space is available for the ligand within the volume occupied by the protein? b) How does the ligand access the active site cavity? c) How completely is the active site cavity filled by the ligand? and d) Which residues in the cavity are close enough to the ligand to provide the anchoring interactions that bind it in place?

Each of these questions involves understanding the shape of the active site cavity, which can be problematic due to self-occlusion of the inner cavity by the outer surface (Figure 2). Dealing with occluded surfaces has long been an area of research in visualization. The next section provides previous work on molecular surface vi-
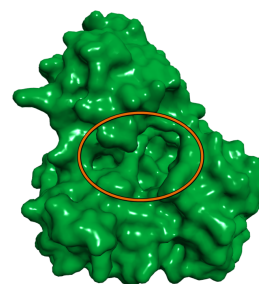

Figure 2: The surface cavity forming the active site of the PGB deaminase enzyme is circled. Much of the cavity is occluded by the outer surface.

sualization, visualizing occluded surfaces, and ambient occlusion.

3   PREVIOUS WORK

3.1   Molecular Surface Visualization

Molecular surfaces are a common visualization technique for studying molecular structures. The solvent-excluded molecular surface is formed by rolling a spherical probe over spheres representing the atoms of the molecule [34]. It represents areas accessible by molecules of a given probe radius. Connolly described methods for generating these surfaces [8, 9]. Methods improving the efficiency and quality of computing these surfaces have also been described [1, 6, 36, 41]. While such methods for producing molecular surfaces are necessary for the visualizations produced in this paper, they do not address the problem of visualizing the occluded interior structure of the generated surfaces.

The problem of visualizing protein docking using surfaces has been addressed [27]. This approach computes the intermolecular negative volume of two docked proteins to determine the amount of intersection between the two surfaces, with the purpose of enhancing drug-design by testing different potential conformations. While effective for such work, this approach is not directly applicable to the biochemistry presented in this paper, which involves data with known structure and no surface intersection.

Methods for analytically extracting pockets and cavities using computational geometry techniques also exist. CASTp uses the weighted Delaunay triangulation and alpha complex to identify and measure the area and volume of pockets and cavities [17], and is available as a PyMOL plugin. The ability to extract measurements of pockets and cavities is very useful, however comparison with an AOOM rendering demonstrates that important features of the cavity may be missed, such as the circled portion of the cavity on the left and the circled access tunnel on the right in Figure 3, Bottom Left (Bottom Right includes a Focal Region technique dis-
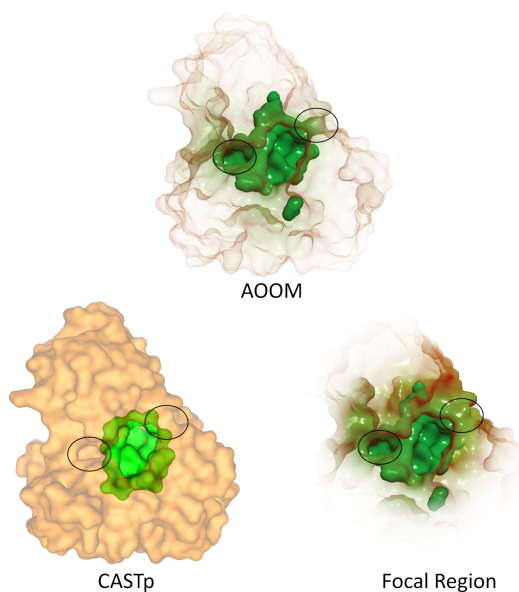
AOOM

CASTp

Focal Region

Figure 3: CASTp cavity extraction (bottom left, rendered using PyMOL) does not extract the entire cavity, and does not conform to the original molecular surface (missing circled regions). A focal-region approach (bottom right) based on distance from the center is less effective than AOOM (top), as it occludes portions of the inner cavity (circled access tunnel on the right) and erodes regions of the outer surface that otherwise provide visual context.

Molecular Surface
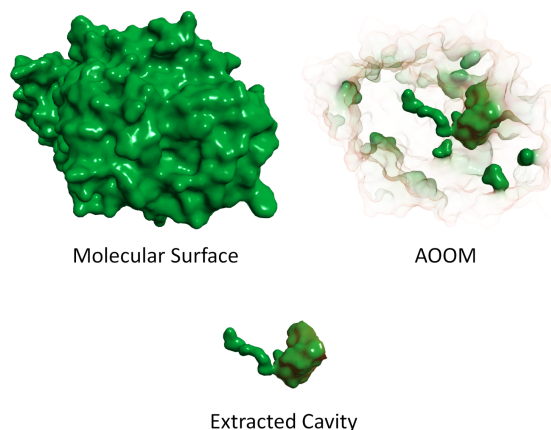

AOOM

Extracted Cavity

Figure 4: A molecular structure [35] (top left) for which CASTp fails, that reveals a long tube-like cavity structure when rendered using AOOM (top right). If desired, the cavity can be extracted by thresholding on ambient occlusion information followed by connected components analysis (bottom).

cussed in Section 3.2), because the cavity is not calculated from the full molecular surface, but instead from the extracted atoms that form the cavity. Also, there are a number of structures for which CASTp fails, whereas AOOM will work for any molecular surface (Figure 4). Future work will include augmenting AOOM with the types of analytical capabilities provided by CASTp. A promising step in this direction involves extracting the cavity by thresholding based on ambient occlusion information, followed by connected components analysis to remove smaller pockets in the surface (Figure 4, Bottom).

Recent work has resulted in techniques for producing simplified abstractions of complicated molecular surfaces [7]. While this technique does not directly address revealing hidden internal structure, it may prove beneficial to combine AOOM with such abstracted surfaces, as AOOM will work with any surface-based representation. Furthermore, AOOM could be applied to other representations, such as ball-and-stick and ribbon renderings.

3.2 Occlusion and Transparency

Occlusion is the most powerful of all depth cues [43]. However, occlusion can be problematic when visualizing 3D data, as objects of interest can be hidden from view. Applying transparency to occluding objects can make hidden objects visible, but simple transparent surfaces do a poor job of conveying surface shape [24]. Various techniques have therefore been developed to enable more effective visualization of occluding and occluded surfaces.

Illustrative Techniques   Illustrative techniques include a surface-rendering technique for view-dependent tranparency that aims to automatically produce transparent surfaces similar to technical illustrations [15]. Later work describes techniques for automatically producing breakaway and cutaway illustrations of nested surfaces [16]. These techniques are useful for nested surfaces, but do not address a single self-occluding surface. Similar work has been applied to isosurfaces extracted from volumetric data [19], which is useful for objects within the volume of the isosurface, but not for a single self-occluding surface.

Focus-and-Context Techniques   A class of direct volume rendering techniques has been developed to reveal the inner structure of volumes while retaining some outer structure to maintain context. Importance-driven volume rendering highlights presegmented regions based on user-supplied importance criteria [42]. Opacity reduction of occluding volumes by finding volumetric features indicating a separation between areas with similar voxel intensities has been described [2, 3]. Selective opacity reduction of regions using a function of shading intensity, gradient magnitude, distance to the eye point, and previously accumulated opacity has also been described [5]. Opacity-peeling can be used to remove some fixed number of fully-opaque layers of material [32]. These focus-and-context techniques use various features of the volumetric data to modulate opacity and reveal hidden structure, and therefore

do not apply directly to molecular surface rendering. A depth-dependent focal region can also be used for opacity modulation [29]. However, applying a similar technique to our data shows that it is insufficient by itself due to the irregular geometries formed by molecular surfaces, even for a relatively round and centralized cavity (Figure 3, Bottom Right). The work of [11] is closest to that described in this paper, as ambient occlusion is also used for modulating opacity. However, their work focuses on volumetric data, and does not perform the smoothing process described in 4.2 (Figure 6 shows AOOM without smoothing).

3.3 Ambient Occlusion

For the techniques listed above, some method of determining the object or volume of interest is necessary, either via distinct and separate surfaces or via functions of the underlying volume. For displaying the inner cavity of a molecular surface, we need a means to determine which portions of the surface constitute the inner cavity of interest. To do so we calculate ambient occlusion for the surface.

Ambient occlusion [4, 26] is a shading method used in computer graphics that approximates complex shadows from an ambient light source by rendering objects darker when surrounded by other objects (Figure 5, Left). The basic algorithm involves casting a number of rays at various angles from each point on a surface, keeping track of the number of rays that intersect another (or the same) surface. Recent work has focused on real-time ambient-occlusion calculation for dynamic scenes [20, 25, 37, 38], but for our static surfaces it is sufficient to use a pre-calculated ray-tracing approach and store the ambient occlusion per-vertex. The ambient occlusion term O_p at a point p on a surface with normal N can be computed by integrating the visibility function V_p over the hemisphere Ω with respect to the projected solid angle:

$$O_p = \frac{1}{\pi} \int_{\Omega} V_p(\vec{\omega})(N \cdot \vec{\omega}) \, d\omega, \quad (1)$$

where $V_p(\vec{\omega})$ is zero if p is occluded in the direction $\vec{\omega}$, and one otherwise. The dot product $N \cdot \vec{\omega}$ results in a cosine-weighting across the hemisphere. Using a cosine-weighted distribution of rays therefore removes the need for this cosine factor, resulting in a simple ratio of the number of rays that intersect a surface r_i and the number of total rays r_t:

$$O_p = \frac{r_i}{r_t}. \quad (2)$$

Areas of the surface that are largely occluded will therefore have a high O_p value.

Ambient occlusion rendering was developed to enhance realism in computer graphics by replacing the standard ambient term by $1 - O_p$ to darken objects blocked from ambient light. Ambient occlusion has also proven useful for scientific visualization. For example, with molecular surface rendering, the locations of cavities in the molecular surface become more apparent (Figure 5, Left). Because ambient occlusion is a measure of the "hiddenness" of a particular point on a surface, we can use ambient occlusion information to identify hidden structures and render them more opaquely to provide visual emphasis.

4 AMBIENT OCCLUSION OPACITY MAPPING

Ambient occlusion opacity mapping (AOOM) uses ambient occlusion information to modulate the opacity of the molecular surface. Areas with high ambient occlusion that would typically be rendered dark, are instead rendered more opaque than areas with low ambient occlusion. The color of the surface can also be adjusted based on ambient occlusion to enhance perception of the inner cavity versus the outer surface. This section describes the implemenation details of AOOM, extensions to the core AOOM technique enabling enhanced opacity control, and supplemental visualization techniques used with AOOM to visualize enzyme-ligand interactions.

4.1 Implementation Details

The examples shown here use surfaces exported from PyMOL. A molecular surface with a probe size of 1.4 Å ($\approx$ radius of water) is used. For most of the examples in this paper, we show PBG deaminase [28] for consistent comparison. Figures 4 and 12 show AOOM applied to other molecules.

We have implemented AOOM via extensions to the Visualization Toolkit (VTK) (www.vtk.org). Surfaces exported from PyMOL are loaded in OBJ or VRML format. Ambient occlusion is pre-computed on the CPU for each vertex on the input via a ray-casting approach, and stored as scalar point data. As with other ray-tracing techniques, calculating per-vertex ambient occlusion is embarrassingly parallel, so we accelerate computation by distributing computation across processing units. Results are typically stored in one of VTK's polygonal file formats so that computation is only necessary once. Because the ambient occlusion is pre-computed, there is a neglible decrease in performance when rendering with AOOM.

Depth sorting is performed to obtain correct blending, which can affect performance for large surfaces, however this is also the case for standard transparency. A depth-peeling approach could also be used to achieve order-independent transparency [14, 18]. Because the O_p term constitutes a scalar field mapped to the surface, a full range of color and opacity functions can be applied, typically in the same fragment program used for lighting and shading. In the simplest case, the opacity
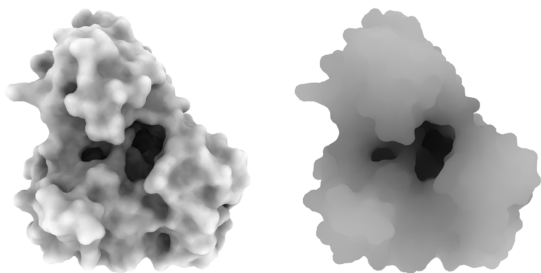
Figure 5: Ambient occlusion (left) vs. smoothed ambient occlusion (right). Using smoothed ambient occlusion for opacity enables filtering of small-scale concavities in the surface.
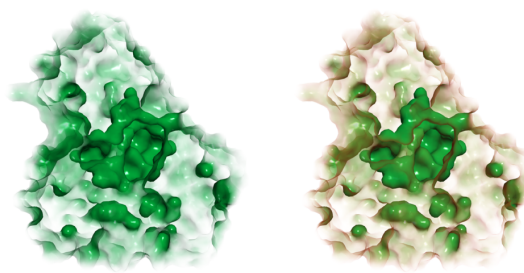

Figure 6: The simplest implementation of AOOM, in which ambient occlusion is directly mapped to opacity. The image on the left uses a constant color, and the image on the right applies a color map to the ambient occlusion.

is set equal to the O_p ambient occlusion term, $\alpha = O_p$, via a linear lookup table, and a constant color is used (Figure 6, Left). A double-ended color map that separates high and low ambient occlusion values can also be applied to help viewers distinguish interior and exterior structures (Figure 6, Right). For the examples in this paper we apply a color map from orange (low ambient occlusion) to green (high ambient occlusion).

This approach is more effective than standard transparency (Figure 1, Left) in revealing the structure of the inner cavity, but can be improved upon with additional opacity controls.

4.2   Smoothed Ambient Occlusion

Although Figure 6 demonstrates an improvement over standard transparency techniques, there are still areas of the outer surface that occlude the interior cavity, due to small concave pockets formed on the surface. To deemphasize these pockets, we smooth the ambient occlusion data over the surface. Smoothing the ambient occlusion filters out small-scale features, while retaining the larger cavity (Figure 5). We smooth the ambient occlusion data directly on the surface by iteratively solving the diffusion partial differential equation:

$$\frac{\partial u}{\partial t} = D \, \nabla^2 u, \qquad (3)$$

where D is a constant controlling the amount of diffusion per time step ($= 1$ in the general case). This approach is equivalent to smoothing using a Gaussian filter, with more iterations equal to a Gaussian with a larger standard deviation. We solve the diffusion equation rather than performing direct convolution with a Gaussian because solving the diffusion equation iteratively only requires sampling immediate neighbors in the polygonal mesh. In practice we have found that 100 iterations works well for our data, and has been used for all images. The smoothing is typically performed once at run-time, upon loading the data.

Although smoothed ambient occlusion is useful for selecting the scale of features that are rendered more

opaquely, we also provide the ability to use the original ambient occlusion for color to retain detail (Figure 8).

4.3   Opacity Control

Arbitrary functions can be used to map the smoothed ambient occlusion values to opacity, however we desire a mapping that maintains the opacity of the inner cavity while providing control over the opacity of the outer surface. We experimented with functions such as *smoothstep*, however the following equation was determined via visual inspection to produce better results:

$$\alpha = \left(\frac{O_p}{\tau} \right)^{\rho}, \qquad (4)$$

where α is clamped to $[0, 1]$. The τ parameter provides a threshold such that an $O_p >= \tau$ gives an α of 1. A τ of 0.7 is used for all images in this paper (other than Figure 6, which uses a simple linear ramp). The ρ parameter controls the shape of the curve as an exponential, and in practice is allowed to vary over $[0, 10]$. For a τ value of 1, a ρ value of 1 will give the same result as the simple linear opacity mapping decribed in section 4.1. Increasing ρ from 1 will reduce the opacity of the outer surface to a greater degree than the inner surface. Decreasing ρ from 1 will increase the overall opacity until ρ reaches 0, resulting in a constant α of 1 and a fully opaque surface. A graphical representation of Equation 4 is shown in Figure 7. The effect of changing ρ is shown in Figure 8, and is typically adjusted interactively by the user.

4.4   Supplementary Visualization Techniques

We also apply a number of supplementary visualization techniques to enable improved understanding of the enzyme active site cavity and ligand.

Silhouette-Edge Highlighting   To maintain contextual information of the outer surface while rendering the interior surface more visible, silhouette-edge highlighting can optionally be applied:

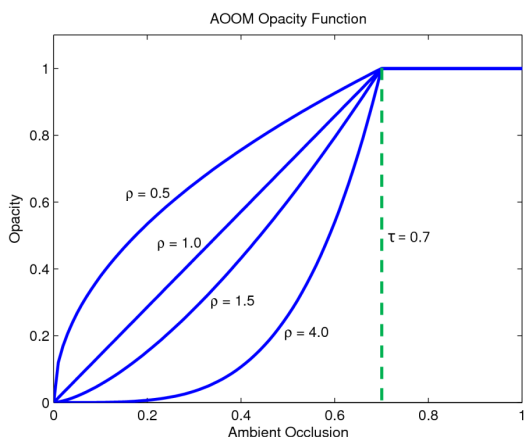$$\alpha = \alpha_{in}^{(\hat{N} \cdot \hat{E} + 1)}, \qquad (5)$$
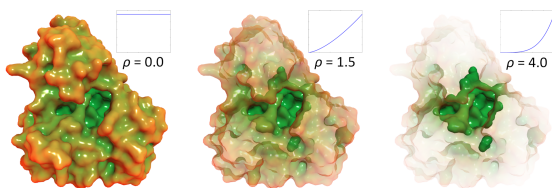
Figure 7: Example AOOM opacity functions.

Figure 8: Result of changing the ρ parameter to adjust outer opacity while maintaining the opacity of the inner cavity.
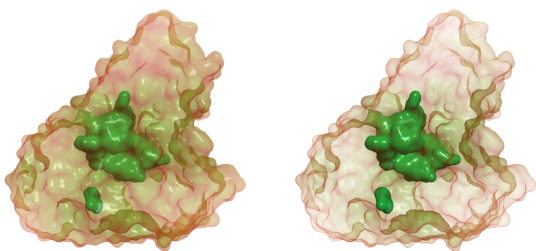

Figure 9: AOOM example without (left) and with (right) silhouette-edge highlighting.

where α_{in} is the opacity after applying Equation 4, and $\hat{N} \cdot \hat{E}$ is the dot product of the surface normal and the eye vector. This equation selectively reduces the opacity of areas on the surface with low opacity that face the viewer. Areas of high opacity are less affected, and areas of full opacity are unaffected. The calculation is performed in the same fragment program used for lighting and AOOM. Other edge highlighting techniques, such as suggestive contours [12, 13], could also be applied. Figure 9 shows the result of applying silhouette-edge highlighting.

Colored Surfaces   To better understand the chemistry occuring in the active site, it can be useful to color the molecular surface by atom type. A nominal color coding is employed, with charged residues colored blue for cationic (positive) species and red for anionic (negative) species. The carbon backbone is colored green in our examples (coloring of specific groups,
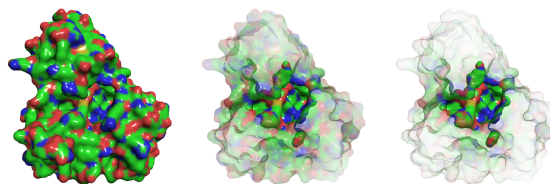

Figure 10: Colored molecular surface (left), along with AOOM renderings without (middle) and with (right) silhouette-edge highlighting.

such as yellow sulfur groups, are also used). Because the molecular surface color conveys information, color mapping as described in Section 4.1 is not desirable in this case, as the nominal color encoding will be distorted. The silhouette-edge highlighting described in above can therefore be especially helpful when using such a color coding (Figure 10).

Enclosed Region Removal   Sometimes fully-enclosed regions are formed during the molecular surface calculation. These regions are not accessible from positions exterior to the enzyme (for molecules with a radius $>=$ the surface probe radius) and can add visual clutter to the scene. These regions can be automatically removed by computing connected components on the molecular surface and rendering only the largest connected component, which will be the main molecular surface (Figure 1, Right vs. Figure 3, Top).

Textured Surfaces   Textured surfaces can help improve surface-shape perception [21, 22]. We therefore apply an optional Perlin noise solid texture [31] to the molecular surface. This can be especially helpful when zoomed in close to the cavity surface (Figure 11).

Ligand Visualization   To understand the interaction between enzymes and ligands, it can be useful to display the ligand within the active site of the enzyme. Figure 11 shows comparison views incorporating stick models of the ligand within the surface cavity, as well as specified enzyme residues of interest. The carbon backbones are colored grey. Other representations of the ligand and residues, such as spheres or van der Waals surfaces, could also be used.

Backface Opacity Modulation   When displaying the ligand within the cavity, portions of the ligand can be obscured within small pockets of the cavity. To enable visualization of the ligand in these areas, further opacity modulation can be applied to render back-facing polygons more transparent (Figure 11). The opacity of back-facing polygons is modulated as:

$$\alpha = \alpha_{in} * \left(1.0 - (\hat{N} \cdot \hat{E}) * C \right), \qquad (6)$$

where α_{in} is the opacity after Equation 4 and optionally Equation 5 are applied, $\hat{N} \cdot \hat{E}$ is the dot product of the surface normal and the eye vector, and C controls the overall opacity reduction. This equation selectively reduces the opacity of back-facing surfaces more
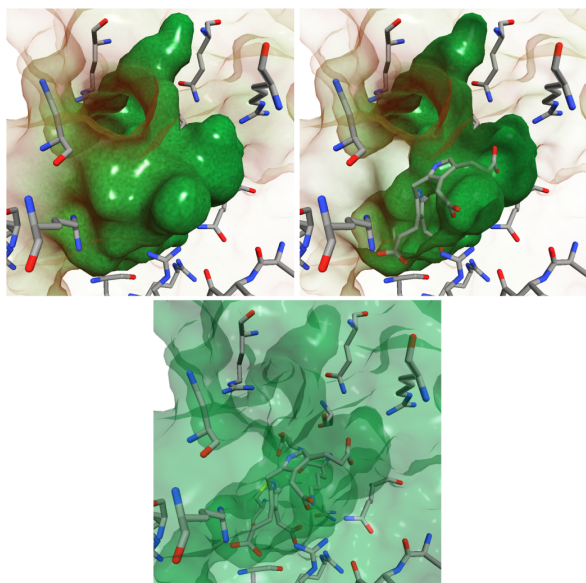
Figure 11: The top views show AOOM renderings of a closeup of the inner cavity. The image on the left shows the back-facing surface with full opacity, and the image on the right shows the back-facing surface rendered with a view-dependent opacity to reveal the ligand within. The bottom image shows the same viewpoint using standard transparency.

where the surface faces the viewer, providing subtle edge highlighting of the back-facing surface. For future work, it may be interesting to apply texture-based transparency methods to back-facing polygons to enable improved perception of the outer and inner surfaces of these pockets [24, 33, 44].

5 CONCLUSION AND FUTURE WORK

We have presented ambient occlusion opacity mapping (AOOM), a novel technique for viewing inner molecular surface structure. AOOM uses ambient occlusion information, a measure of the "hiddenness" of a particular point on a surface, to render occluded areas of a surface more opaque than non-occluded areas. We have shown the application of AOOM to the specific problem of visualizing the active sites of enzymes, as our collaborators have successfully used AOOM to better understand the structure of this inner cavity. Smoothing the ambient occlusion information over the surface enables control over the scale of the cavities to highlight. Color and opacity controls, including silhouette-edge highlighting, have also proven useful in highlighting the inner cavity of interest. AOOM is more effective than techniques such as transparency, clipping planes, and focal regions, and works for cases where cavity extraction techniques such as CASTp fail.

We have implemented AOOM via extensions to the Visualization Toolkit (VTK), and have created a test
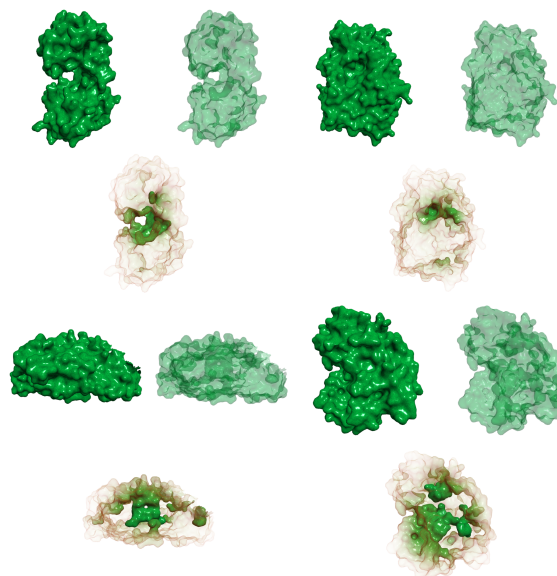

Figure 12: Various enzymes rendered using AOOM (bottom) to enable better perception of inner structure than with standard transparency (top right).

application using this code. Future work includes incorporating AOOM into existing molecular visualization packages, such as PyMOL, to take advantage of features, including measurements and ribbon-style rendering, that our collaborators already find useful.

It may also prove useful to apply AOOM in fields other than molecular visualization. Specifically, medical visualization and oil and gas visualization could benefit from AOOM, as both fields often work with data sets exhibiting inner structures of interest that may be occluded.

6 ACKNOWLEDGMENTS

REFERENCES

[1] Jean-Daniel Boissonnat, Olivier Devillers, and Jacqueline Duquesne. Computing Connolly surfaces. *J. Molecular Graphics*, 12(1):61–62, 1994.

[2] David Borland. *Flexible Occlusion Rendering for Improved Views of Three-Dimensional Medical Images*. PhD thesis, Department of Computer Science, University of North Carolina at Chapel Hill, 2007.

[3] David Borland, John P. Clarke, Julia R. Fielding, and Russell M. Taylor II. Volumetric depth peeling for medical image display. In Robert F. Erbacher, Jonathan C. Roberts, Matti T. Gröhn, and Katy Börner, editors, *Visualization and Data Analysis, Proceedings of SPIE-IS&T Electronic Imaging 2006*, volume 6060, pages 35–45, January 2006.

[4] Rob Bredow. Renderman on film: Combining CG and live action, Course 16: RenderMan in Production. In *ACM SIGGRAPH 2002 Course Notes*, 2002.

[5] Stefan Bruckner, Sören Grimm, Armin Kanitsar, and M. Eduard Gröller. Illustrative context-preserving exploration of volume data. *IEEE Transactions on Visualization and Computer Graphics*, 12(6):1559–1569, 2006.

[6] Ho-Lun Cheng and Xinwei Shi. Quality mesh generation for molecular skin surfaces using restricted union of balls. In *Proceedings of IEEE Visualization*, pages 399 – 405, 2005.

[7] Gregory Cipriano and Michael Gleicher. Molecular surface abstraction. *IEEE Transactions on Visualization and Computer Graphics*, 13(6):1608–1615, 2007.

[8] Michael L. Connolly. Solvent-accessible surfaces of proteins and nucleic acids. *Science*, 221(4612):709–713, 1983.

[9] Michael L. Connolly. The molecular surface package. *J. Molecular Graphics*, 11(2):139–141, 1993.

[10] Michael L. Connolly. Molecular surfaces: A review. *Network Science*, online article http://www.netsci.org/Science/Compchem/feature14.htm, 1996.

[11] Carlos Correa and Kwan-Liu Ma. The occlusion spectrum for volume classification and visualization. *IEEE Transactions on Visualization and Computer Graphics*, 15(6):1465–1472, 2009.

[12] Doug DeCarlo, Adam Finkelstein, and Szymon Rusinkiewicz. Interactive rendering of suggestive contours with temporal coherence. In *Proceedings of the 3rd international symposium on Non-photorealistic animation and rendering*, pages 15–24, 2004.

[13] Doug DeCarlo, Adam Finkelstein, Szymon Rusinkiewicz, and Anthony Santella. Suggestive contours for conveying shape. In *Proceedings of SIGGRAPH*, pages 848–855, 2003.

[14] Paul J. Diefenbach. *Pipeline rendering: Interaction and realism through hardware-based multi-pass rendering*. PhD thesis, Department of Computer Science, University of Pennsylvania, 1996.

[15] Joachim Diepstraten, Daniel Weiskopf, and Thomas Ertl. Transparency in interactive technical illustration. *Computer Graphics Forum*, 21(3):317–325, 2002.

[16] Joachim Diepstraten, Daniel Weiskopf, and Thomas Ertl. Interactive cutaway illustrations. *Computer Graphics Forum*, 22(3):523–532, 2003.

[17] Joe Dundas, Zheng Ouyang, Jeffery Tseng, Andrew Binkowski, Yaron Turpaz, and Jie Liang. CASTp: Computed atlas of surface topography of proteins with structural and topographical mapping of functionally annotated residues. *Nucleic Acids Research*, 34:W116–W118, 2006.

[18] Cass Everitt. Interactive order-independent transparency. Technical report, Nvidia Corporation, 2002.

[19] Jan Fischer, Dirk Bartz, and Wolfgang Strasser. Illustrative display of hidden iso-surface structures. In *Proceedings of IEEE Visualization*, pages 663–670, 2005.

[20] Athanasios Gaitatzes, Yiorgos Chrysanthou, and Georgios Papaioannou. Presampled visibility for ambient occlusion. *Journal of WSCG*, 16(1-3):17–24, 2008.

[21] James J. Gibson. *The Perception of the Visual World*. Houghton Mifflin, 1950.

[22] James J. Gibson. *The Ecological Approach to Visual Perception*. Houghton Mifflin, 1979.

[23] David S. Goodsell. Visual methods from atoms to cells. *Structure*, 13(3):347–354, 2005.

[24] Victoria Interrante, Henry Fuchs, and Stephen M. Pizer. Conveying the 3D shape of smoothly curving transparent surfaces via texture. *IEEE Transactions on Visualization and Computer Graphics*, 3(2):98–117, 1997.

[25] Adam G. Kirk and Okan Arikan. Real-time ambient occlusion for dynamic character skins. In *Proceedings of the ACM SIGGRAPH Symposium on Interactive 3D Graphics and Games*, April 2007.

[26] Hayden Landis. Production-ready global illumination, Course 16: RenderMan in Production. In *ACM SIGGRAPH 2002 Course Notes*, 2002.

[27] Chang Ha Lee and Amitabh Varshney. Computing and displaying intermolecular negative volume for docking. In G. M. Nielson G.-P. Bonneau, T. Ertl, editor, *Scientific Visualization: The Visual Extraction of Knowledge from Data*. Springer-Verlag, ISBN 3-540-26066-8, 2005.

[28] G. V. Louie, P. D. Brownlie, R. Lambert, J. B. Cooper, T. L. Blundell, S. P. Wood, M. J. Warren, S. C. Woodcock, and P. M. Jordan. PDB #: 1pda: Structure of porphobilinogen deaminase reveals a flexible multidomin polymerase with a single catalytic site. *Nature*, 359:33–39, 1992.

[29] Rakesh Mullicka, R. Nick Bryanb, and John Butmana. Confocal volume rendering: Fast segmentation-free visualization of internal structures. In Seong K. Mun, editor, *Medical Imaging 2000: Image Display and Visualization*. Proceedings of SPIE, SPIE Vol. 3976, 2000.

[30] Arthur J. Olson and Michael E. Pique. Visualizing the future of molecular graphics. *SAR and QSAR in Environmental Research*, 8(3-4):233–247, 1998.

[31] Ken Perlin. Improving noise. *Computer Graphics*, 35(3), 2002.

[32] Christof Rezk-Salama and Andreas Kolb. Opacity peeling for direct volume rendering. *Computer Graphics Forum*, 25(3):597–606, 2006.

[33] Penny Rheingans. Opacity-modulating triangular textures for irregular surfaces. In *Proceedings of IEEE Visualization*, pages 219–225, 1996.

[34] Frederic M. Richards. Areas, volumes, packing and protein structure. *Annual Review of Biophysics and Bioengineering*, 6:151–176, 1977.

[35] E. H. Rydberg, C. Li, R. Maurus, C. M. Overall, G. D. Brayer, and S. G. Withers. PDB #: 1kbb: Mechanistic analyses of catalysis in human pancreatic alpha-amylase: detailed kinetic and structural studies of mutants of three conserved carboxylic acids. *Biochemistry*, 41(13):4492–4502, April 2002.

[36] Michel F. Sanner, Arthur J. Olson, and Jean-Claude Spehner. Fast and robust computation of molecular surfaces. In *Proceedings of the eleventh annual symposium on Computational geometry*, pages 406 – 407, 1995.

[37] Perumaal Shanmugam and Okan Arikan. Hardware accelerated ambient occlusion techniques on GPUs. In *Proceedings of the ACM SIGGRAPH Symposium on Interactive 3D Graphics and Games*, pages 73–80, April 2007.

[38] Peter-Pike Sloan, Naga K. Govindaraju, Derek Nowrouzezahrai, and John Snyder. Image-based proxy accumulation for real-time soft global illumination. In *Proceedings of the 15th Pacific Conference on Computer Graphics and Applications*, pages 97–105, 2007.

[39] Marco Tarini, Paolo Cignoni, and Claudio Montani. Ambient occlusion and edge cueing to enhance real time molecular visualization. In *Proceedings of IEEE Visualization*, 2006.

[40] John Tate. Molecular visualization. In Philip E. Bourne and Helge Weissig, editors, *Structural Bioinformatics*, chapter 23. Wiley-Liss, 2003.

[41] Amitabh Varshney and Jr. Frederick P. Brooks. Fast analytical computation of richard¿½s smooth molecular surface. In *Proceedings of IEEE Visualization*, pages 300–307, 1993.

[42] Ivan Viola, Armin Kanitsar, and Meister Eduard Gröller. Importance-driven volume rendering. In *Proceedings of IEEE Visualization*, pages 139–146, 2004.

[43] Colin Ware. *Information Visualization: Perception for Design*. Morgan Kaufmann Publishers, second edition, 2004.

[44] Chris Weigle and Russell M. Taylor II. Visualizing intersecting surfaces with nested-surface techniques. In *Proceedings of IEEE Visualization*, pages 503–510, 2005.